Synthesis of AAO Nanotemplate and Its Properties

Natalia TSYNTARU*, Berkay KAVAS**, Jean-Pierre CELIS*
* *Katholieke Universiteit Leuven, Leuven, Belgium*
***Istanbul Technical University, Istanbul, Turkey*
Natalia.Tintaru@mtm.kuleuven.be

***Abstract* – The objective of this study is to synthesize and to characterize anodized aluminium oxide (AAO) nano-templates suited for large area device applications. The wear performance and the mechanical properties of well-ordered nanoporous AAO obtained after a two step anodizing process in sulphuric acid were investigated. Pores with different aspect ratios were obtained at cell voltages of 15 V and 21V. Ppore diameters of ~16 nm and ~ 27 nm were noticed. The mechanical behaviour of such anodized aluminium oxides (AAO) was determined by nanoindentation at 2 -200mN normal loads. The tribological behaviour of these nano-templates was studied under reciprocating (ball on flat) sliding against alumina counter-balls. The dependence of the properties of AAO-templates on the small pore diameter is discussed**

***Index Terms* – anodized aluminium oxide; friction and wear; hardness; pore diameter.**

I. INTRODUCTION

Due to the rapid development in nanotechnologies, a lot of attention is given to the preparation and characterization of anodic aluminium oxide (AAO) membranes. AAO is a nanostructured material which can be of interest in many fields like catalysis, chemical sensors, biosensors, filters, templates for self-assembly, and humidity sensors [1, 2]. The AAO film can also be used as a support for measuring mechanical properties of nanocarbon tube ropes [3]. AAO films are potentially advantageous for tribological applications since the nanoporous structure can be used as a reservoir or a template for solid lubricants and nano-tubes or nano-fibers to form self lubricating structures [4]. AAO microstructures can be classified into two types: a relatively pure alumina type (inner layer) consisting entirely of Al_2O_3, and an acid anion-contaminated type (outer layer) resulting from the incorporation of anions into the alumina structure during anodizing [5]. These phases present in the AAO structures are important when using AAO membranes in applications requiring a high mechanical strength. Friction and wear performance of filled-in AAO films were previously studied [6].

However, a better understanding of wear and friction properties of AAO and how the behaviour of AAO changes with further processing, are still needed. In this investigation, AAO films have been synthesized with narrow pores, and tribological and mechanical studies of these AAO films supported by an aluminium substrate have been performed.

II. EXPERIMENTAL

2.1 Sample preparation

Prior to anodizing, commercial pure Al sheet (% 99.99, Alfa Aesar Johnson Matthey GmbH) was cut into round pieces with a diameter of 9 mm that perfectly match in a sample holder. Samples were ultrasonically degreased in acetone and ethanol followed by a rinsing with deionised water. Anodizing was done on a surface with low roughness. Hereto aluminium samples were electropolished at a constant current density of 500 $mA.cm^{-1}$ for 1 min in an electrolyte consisting of perchloric acid (60 wt %) and ethanol (abs.) in a volumetric ratio of 1:4. Temperature was kept at ~10 ^oC [7, 8]. [9]. Perchloric acid was used to achieve the proper low pH and to ensure that Al ionizes into Al^{3+} and does not form oxides [10]. It must be noted that the edges of the sample were electrically isolated.

2.2. Anodizing

Two step anodizing was performed in a 20 wt % sulphuric acid electrolyte using a two electrode electrochemical cell set up with a magnetic stirrer rotating at 500 rpm. The temperature was kept at ~ 1 ^oC during anodizing. Electropolished samples were cleaned in de-ionized water and anodised at a potential of either 15 or 21V for 10 min. After a first anodizing step, samples were rinsed with de-ionized water and immersed in a solution of chromic acid (1.8 wt%) and phosphoric acid (6 wt %) for 10 and 15 min respectively, at ~60 $^{\circ}C$ to achieve a removal of the oxide layer. In this way, we achieved a prepatterning of the aluminium surface for pores to grow inwards during the second anodizing step at a constant potential of either 15 or 21 V for 97 and 20 min respectively at ~ 1 $^{\circ}C$. The AAO thickness was ~17 µm (Fig.1.). Pore sizes 16 and 27 nm.

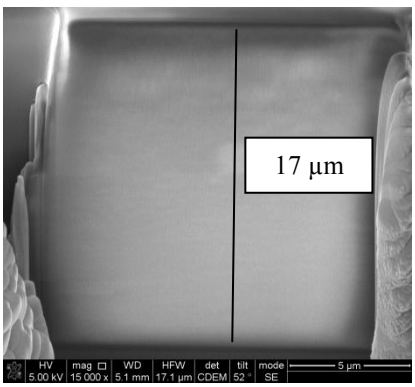

Fig.**1.** Cross section on AAO with a thickness of 17 µm (light grey area: AAO, dark grey area Al).

2.3. Tribological and mechanical characterisation

For the investigation of tribological properties at meso- and macro-loads, we used Falex Modular Universal Surface Tester (MUST) and a KUL-MTM fretting mode I apparatus [11]. The counterbody was a 5 mm corundum ball reciprocating on AAO samples at a frequency of 1 Hz. The stroke length was 100 µm. Tests were repeated at least three times at normal loads between 40 mN and 1,000 mN to reveal the tribological behaviour at low and rather high loads. Test temperature was kept constant at 23°C. Humidity was 50% RH. Samples were cleaned before fretting tests for degreasing them, and after fretting tests ultrasonically in ethanol for 7-10 min to remove the debris. Samples were examined using scanning electron microscopy (SEM, Philips XL-30), Field Ion Beam SEM (FIB-SEM) and white light interferometer (VeeCo) before and after wear tests. Chemical composition was identified by energy-dispersive spectroscopy (EDS).

Nanoindentation was performed at six different loads as 2, 5, 20, 50, 100 and 200 mN using Berkovich nanoindenters (CSM Instruments). Loading and unloading rates were as twice as the maximum load applied. Indentation marks were examined by optical microscopy and SEM.

III. RESULTS AND DISCUSSION

3.1. Influence of sample preparation procedure

The anodizing of aluminium was done on samples with a low surface roughness. Indeed, anodising reactions take place at the surface of the anode, and a low surface roughness is a must to get a uniform anodizing rate at each spot. SEM and white light interferometer investigation performed before and after electropolishing, revealed how this pre-treatment influences the surface roughness. Roughness values, Ra and Rz were ~740 nm and ~7 µm prior to electropolishing. After electropolishing Ra and Rz were ~140 nm and ~1.5 µm respectively. SEM images of the two types of surfaces are given in Fig.2.

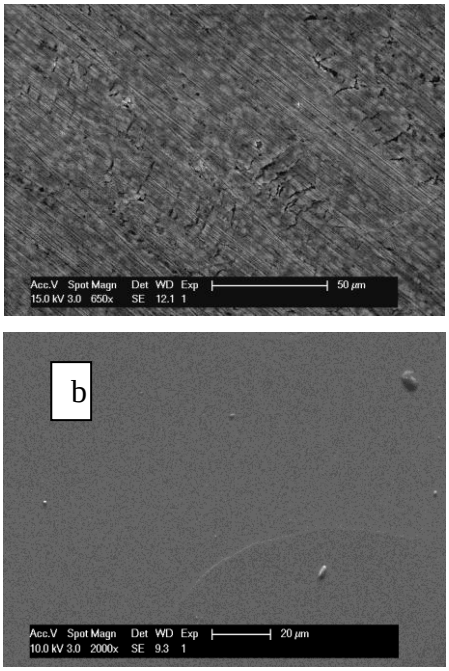

Fig. 2. SEM images of the aluminium surface before (a) and after electropolishing (b).

3.2. Tribological performance of as-received AAO films

In order to determine the tribological behaviour of amorphous [5] as-produced AAO films supported on aluminium substrate, fretting test were carried out. The evolution of the coefficient of friction with fretting cycles is given in Fig. 3. It shows the dependence of the coefficient of friction on the pore diameter and normal load applied. The coefficient of friction increases steeply at the beginning of the sliding tests. After around 80-100 cycles at meso-loads, a steady state is reached during which the coefficient of friction is approximately the same for both pore sizes. The coefficient of friction for AAOs with the same pore diameter, remained practically the same independently the load applied. At high loads of 1,000 mN, the coefficient of friction is higher probably due to of debris formed during the fretting tests. At a smaller AAO pore diameter namely 16 nm, this effect is more obvious (Fig. 3a). Since we used a counterbody also made of alumina, the coefficient of friction can reach high values, but it also assures that no chemical reaction will occur in the sliding contact. However, after reaching a peak value, the coefficient of friction decreases slightly especially at a normal load of 1,000 mN (Fig. 3).

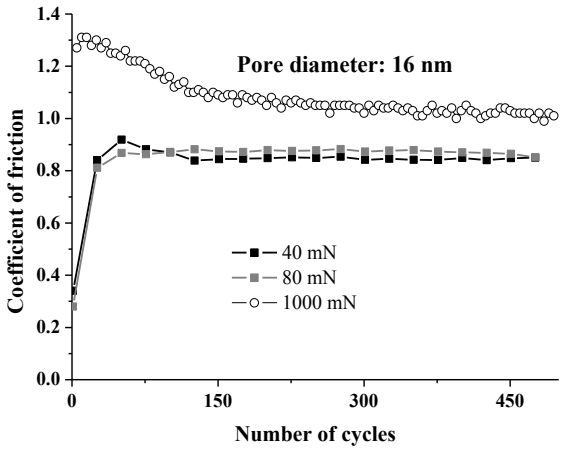

Fig. 3. Evolution of AAO coefficient of friction at meso- and macroscale loads.

To reveal the wear mechanism during the running-in period, short sliding tests of 50 cycles were done. Wear tracks observed using SEM (Fig.4) revealed that the pores were filled up with very fine debris formed in the sliding contact. Some pores could still partially be seen underneath a very thin debris layer covering the surface. It can be noticed that the pores were obtained without any serious damage to the tubes.

To study the propagation of wear, wear tracks after 500 fretting cycles (steady state part) were analyzed (Fig 5). These experiments show that a tribolayer is formed by a progressive degradation of the AAO top layer and by filling up the pores with nanosized debris. This tribolayer consists of a compacted bed of wear particles and has a partially layered structure which we observed after 500 fretting cycles. That tribolayer is not equally spread over the whole wear track area (Figures 4 and 5).

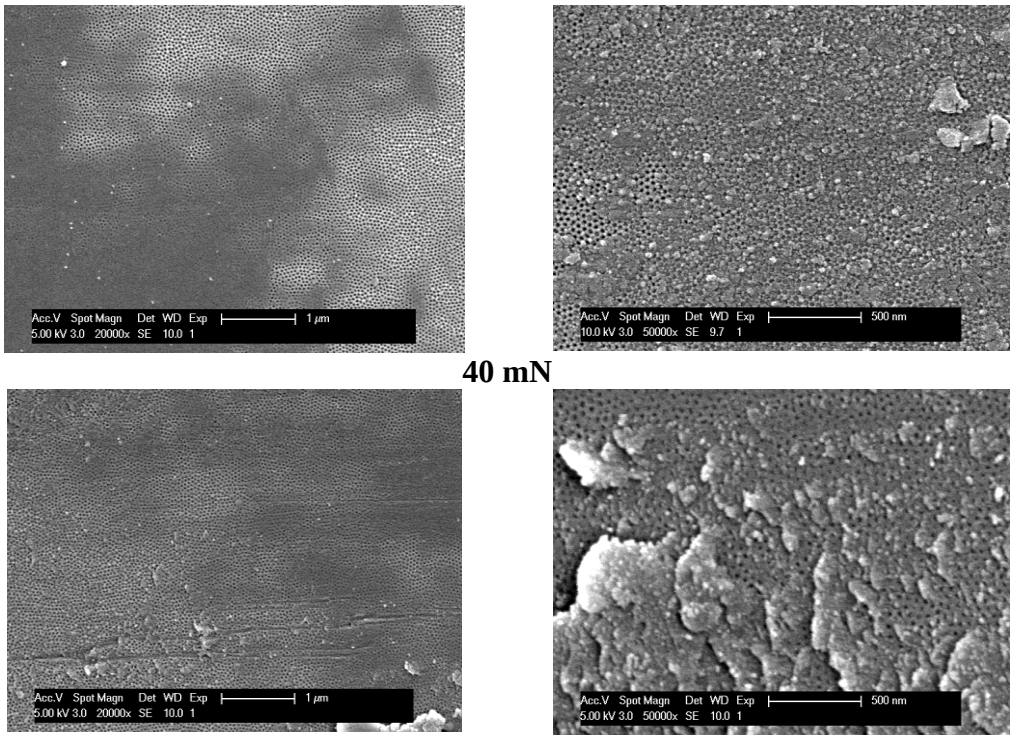

Fig. 4. SEM images of AAO (pore diameter 27 nm) after 50 fretting cycles.

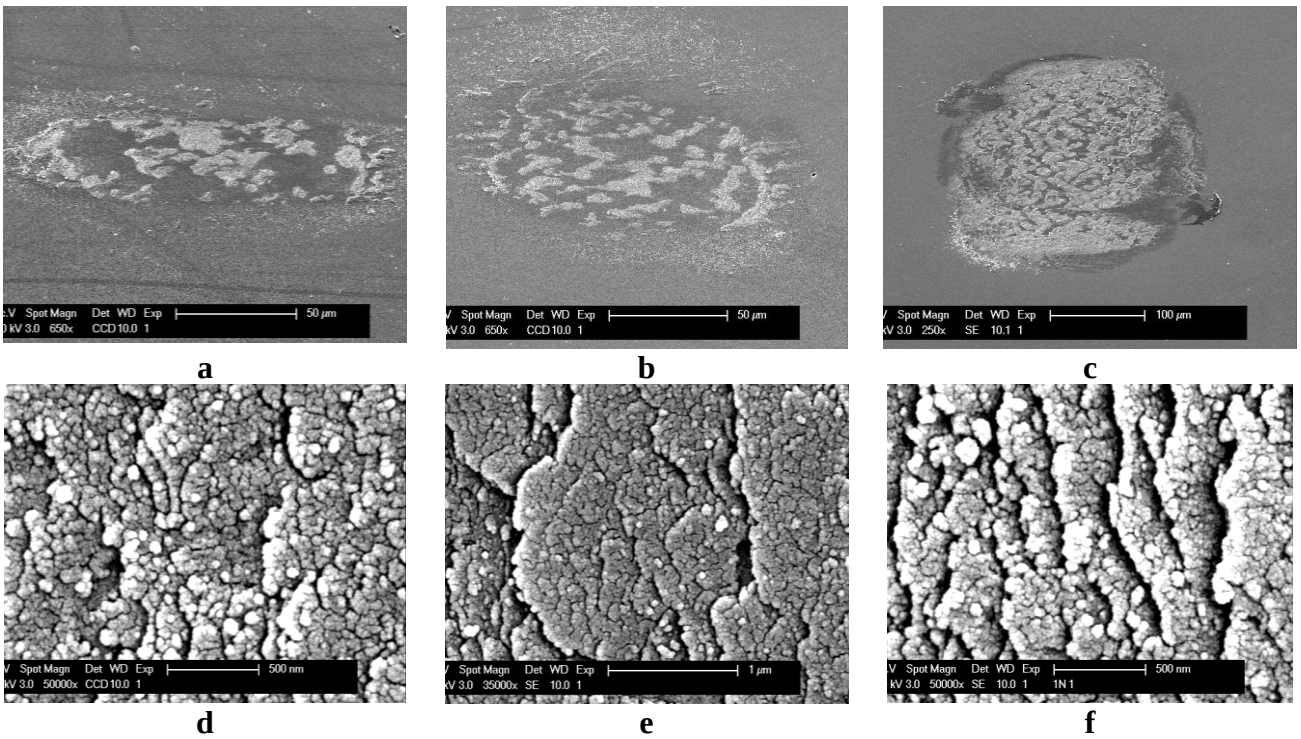

Fig. 5. SEM images of wear tracks on AAO membrane (pore diameter 27nm) after 500 sliding cycles at normal loads of 40, 80 and 1000 mN at low magnification (a, b and c) and high magnification (d, e and f) respectively

Ultrasonic cleaning of the tested samples in ethanol after the wear tests, did not allow to remove the bed of debris from the surface. This reveals that the debris iss sticky, adhering locally on some parts of the wear track and on the counterbody (not shown here), resulting in a complex wear mechanism being a combination of abrasive and adhesive wear, and in a high coefficient of friction. The increasing coefficient of friction at the start of the sliding tests can be linked to the formation of this tribolayer. On further sliding, compacted small worn debris may cause abrasion wear and a high coefficient of friction.

3.2. Nanoindentation

Nanoindentation tests were performed over a wide range

of normal loads (2-200 mN) to study the mechanical behaviour of anodized aluminium oxides. The investigation of nanoindentation imprints and surrounding areas was done by using SEM. The study did not reveal major cracks inside and outside the indentation imprints (Fig. 6). Considering that alumina is a ceramic material, the actual mechanism of deformation within the material during indentation comes into question. A high magnification SEM image of an indentation in an AAO film is shown in Fig. 6, in which a pore crushing is evident as the mechanism caused permanent deformation in the material. The corner of the imprint seen in Fig. 6, is surrounded by a regular pore structure, while the pores appear to be deformed within the imprint due to an overall collapse of the porous structure. Rather than through pure material plasticity, the overall structure of the AAO membranes is progressively deformed on indenter loading.

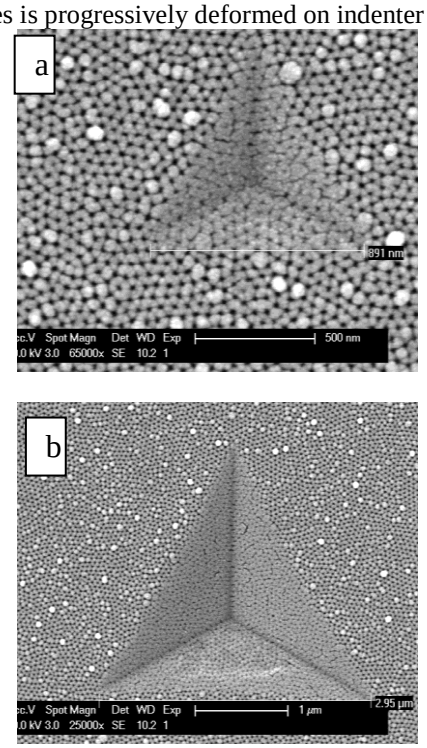

Fig. 6. Nanoindentation imprints at 2, 20 mN (a and b) respectively and surrounding area on AAO templates at pore diameter 27 nm.

Data on hardness and elastic modulus are plotted in Fig.8 versus indentation depth. At low indentation depth, a large scatter in hardness (e.g. 9.5±0.8 GPa and 5.4±0.5 GPa for 2mN, Fig.7 a) and elastic modulus (97±5 GPa for 2mN Fig.7 b) are observed. It is noticed that at on AAO with a 16 nm pore diameter, the scatter is large. This scatter may be due to the high surface roughness and the presence of different structures (such as remains of electrolytes) inside the pores. At large indentation depth, hardness and elastic modulus exhibit a lower scatter. The hardness varies between 3 and 6 GPa and the elastic modulus between 30 and 65 GPa. The hardness and Youngs' modulus of AAO nanotemplate are in good agreement with values reported by other researchers [12]. However, the values are significantly lower than the values found in literature for pure, well crystalline corundum or sapphire, which are usually in the range between 20 and 25 GPa [13]. This difference is mainly attributed to the porous structure, which is responsible for the unique mechanical response of the membranes.

It is noticed that with increasing pore diameter, the hardness at low loads are smaller which can be linked to the 'hole effect' described in [14]. This research shows that the elastic modulus and hardness vary when the normal load is increased. The difference is thought to be due to the anisotropy which is not accounted for in the indentation method and also due to the influence of the aluminium substrate underneath the AAO film.

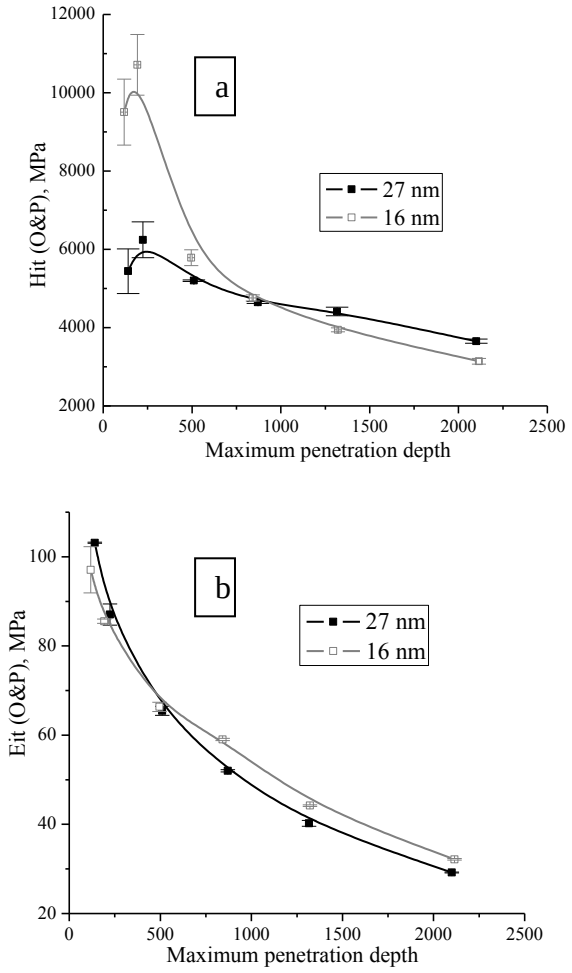

Fig. 7. Hardness (a) and elastic modulus (b) as a function of indentation depth recorded on 17 µm thick AAO membrane produced at 15 and 21 V.

IV. CONCLUSION

Well-ordered nanoporous AAO film was obtained with relative small pore diameters of 16 and 27 nm. It was been shown that AAO films subjected to meso- and macro-load fretting tests form very fine debris on their surface. Debris produced during sliding on the surface fill up the pores in a first stage, followed by the formation of a tribolayer.

Major cracks were not observed inside or along the edges of the wear tracks. Cracks which formed during fretting at 1000 mN don't propagate and are only located at the edges of the wear track. This effect can be linked to the aluminium supporting the AAO template and which is a softer material than the AAO film. The variation in the coefficient of friction with pore size and normal load was not considerably high. The wear mechanism did not change with increasing applied loads due to a similarity in the tribofilm formed under meso- and macro-load sliding testing.

Hardness and Young's modulus of highly ordered alumina were measured by nanoindentation. The hardness and elastic modulus values depend on the load applied. Hardness can reach up to 10 GPa at 2 mN on AAO films

with a 16 nm pore diameter. At increasing loads the nanopores collapse in 'shear bands', rather than being cracked as observed around the indent, suggesting that the pores in the alumina lead to a higher toughness in the transverse direction.

ACKNOWLEDGMENTS

This research was funded by a FP7 grants: "NANOALLOY" (Marie Curie IIF contract n° 252407), "NANOCOAT" (FP7-SME-2010 contract n°262078), and "TEMADEP" (IRSES contract n° 05-104-7540).

REFERENCES

[1] M. Almasi Kashi, A. Ramazani, M. Raoufi, A. Karimzadeh, Thin Solid Films 518, 6767-6772, 2010

[2] Te-Hua Fang, Tong Hong Wang, Chien-Hung Liu, Liang-Wen Ji, Shao-Hui Kang, Nanoscale Res Lett 2, 410-415, 2007

[3] J.-P. Salvetat, G. Andrew, D. Briggs, J.-M. Bonard, R.R. Bacsa, A.J. Kulik, T. Stöckli, N.A. Burnham and L. Forró, Phys. Rev. Lett. 82, 944. 1999

[4] H. Kim, D. Kim, W. Lee, S. Jai Cho, J.-H. Hahn, and H.-S. Ahn, Surf. Coatings Techn., doi:10.1016/j. surfcoat.2010.07.056, in Press.

[5] M. Kylan McQuaig Jr., Alejandro Toro, William Van Geertruyden, Wojciech Z. MisiolekJ, Mater Sci 46, 243–253, 2011

[6] J.P. Tua, C.X. Jiang, S.Y. Guoc, X.B. Zhaoa, M.F. Fu, Wear 259, 759–764, 2005

[7] G.D. Sulka, S. Stroobants, V. Moschalkov, G. Borghs, and J.-P. Celis, J. Electrochem. Soc., 149 (7), D97-D103, 2002

[8] G.D. Sulka, K. G. Parkola, Thin Solid films, 515, 338–345, 2006

[9] H. Adelkhani, S. Nasoodi, A.H. Jafari, Int. J. Electrochem. Sci., 4, 238 – 246, 2009

[10] Di Ma, Shuying Li, Chenghao Liang, Corrosion Science 51, 713-718, 2009

[11] H. Mohrbacher, J.-P. Celis and J.R. Roos, Tribo. Int., 28 (5), 296-278, 1995

[12] Z. Xia, L. Riester, B. W. Sheldon, W. A. Curtin, J. Liang, A. Yin and J. M. Xu, Rev.Adv.Mater.Sci., 6, 131-139, 2044

[13] AB Sinani, NK Dynkin, LA Lytvinov, PV Konevsky, EP Andreev, Bull Russ Acad Sci Phys, 73, 1380, 2009

[14] S. Ko et al., Thin Solid Films 515, 1932–1937, 2006